Hydrol. Earth Syst. Sci. Discuss., 9, 4919–4941, 2012
www.hydrol-earth-syst-sci-discuss.net/9/4919/2012/
doi:10.5194/hessd-9-4919-2012

Hydrology and Earth System Sciences Discussions

Factors affecting the runoff coefficient

G. Del Giudice, R. Padulano, and G. Rasulo

Federico II University, Department of Hydraulic, Geothecnical and Environmental Engineering, Via Claudio 21, 80125, Naples, Italy

Received: 31 March 2012 – Accepted: 4 April 2012 – Published: 17 April 2012

Correspondence to: G. Del Giudice (delgiudi@unina.it)

Published by Copernicus Publications on behalf of the European Geosciences Union.

Title Page
Abstract | Introduction
Conclusions | References
Tables | Figures
◀◀ | ▶▶
◀ | ▶
Back | Close
Full Screen / Esc
Printer-friendly Version
Interactive Discussion

Abstract

The runoff coefficient φ is a crucial parameter for flood peak discharge estimate in ungauged drainage basins. Tables and graphs generally allow the determination of φ in a somewhat empirical way that can lead to inconsistency in application; therefore, it is important to identify other parameters that can be utilized to assess φ more directly.

In the present paper, focusing on Southern Continental Italy, a simple analytical expression between runoff coefficient φ and soil potential maximum retention S is proposed; moreover, an improvement of this expression is provided by considering the pre-event moisture condition of the watershed through the use of a climatic factor. At this aim, the US Soil Conservation Service classification for soil permeability has been adopted, that allows the evaluation of S, according to its relationship with the runoff curve number CN, as a function of soil type, land use and antecedent soil moisture condition (AMC).

1 Introduction

One of the most commonly adopted methods for regional flood frequency analysis is the "index flood" (Darlymple, 1960; Riggs, 1973); in accordance with it and whatever statistical method is used to evaluate its probability distribution, the annual maximum flood-peak discharge Q_T, with return period T, can be written as:

$$Q_T = \xi_Q K_T \quad (1)$$

where (i) ξ_Q is the index flood of the examined site, usually the mean or modal value, depending on the probability distribution model used, and (ii) K_T is a dimensionless growth factor, related to the return period and to the adopted probability model.

Hydrological similitude criteria (Penta et al., 1972; Rossi et al., 1982; Cunnane, 1988; Hoskings et al., 1997) are based on the identification of homogeneous regions within which the probability distribution of annual maximum flood peak discharge is invariant (uniqueness of the growth factor K_T), whereas the index flood, representing the scale factor, depends on the characteristics of each watershed.

Therefore, for basins where no direct measurements are available, the main technical problem is to evaluate the flow index ξ_Q. One of the most popular methods literature provides to estimate the index flood in ungauged watersheds is the kinematic runoff model (Eagleson, 1972), whose physically based relation is:

$$\xi_Q = \frac{\varphi \cdot I_A(A,d,T) \cdot A}{3.6} \tag{2}$$

where: (i) ξ_Q is the index flood (in $m^3 s^{-1}$); (ii) A is the watershed area (in km^2); (iii) I_A (A, d, T) is the mean rainfall intensity over the basin (in $mm\,h^{-1}$), whose return period T is the same as the index flood, and whose duration, d, is equal to the concentration time T_C of the watershed; (iv) φ is the runoff coefficient, that is the ratio between effective and total rainfall.

In order to estimate the Intensity-Duration-Frequency (IDF) Curves, representing the maximum point rainfall intensity I_P (d, T) as a function of duration d and return period T (Koutsoyiannis et al., 1998), many methods can be applied (Chow et al., 1998). Conversely, only a few empirical relations are available in literature (Eagleson, 1972) for Areal Reduction Factor (ARF) estimate, namely the ratio between I_A (A, d, T) and I_P (d, T):

$$\mathrm{ARF}(A,d,T) = \frac{I_A(A,d,T)}{I_P(d,T)} \tag{3}$$

Moreover, a large number of empirical relations can be applied to evaluate T_C in accordance with watershed geo-morphological features (Chow et al., 1998), whereas tables and graphs allow the determination of φ from different parameters assumed as representative of watershed soil permeability. Because of the above mentioned multiple choices, results can be very different depending on the various formulas and tables adopted, which are quite different from each other.

HESSD
9, 4919–4941, 2012

In the present paper, using the annual maximum flood-peak discharge data of river gauging stations within the Southern Continental Italy watersheds, some analysis are provided in order to obtain the main factors affecting the runoff coefficient φ as well as to propose a simple analytical expression for its better estimation within ungauged basins.

2 Data sources

The annual peak flood values were taken from "Pubblicazione n.17" published by the SIMN (Servizio Idrografico e Mareografico Nazionale) for the gauged river sections located within the river basins of Southern Continental Italy. These values have been already processed by the Operative Units of National Group for Prevention from Hydro-geological Disasters (GNDCI), within the special project on "Flood Evaluation" (VAPI) supported by the National Research Council (CNR) of Italy. The data reliability tests allowed to reject some data in addition to those already eliminated within the VAPI project. Indeed, in some cases it was found that some drainage basins presented an anomalous unit discharge ($m^3 s^{-1} km^2$) if compared to the watersheds belonging to the same river but situated upstream or downstream.

Table 1 shows, for each region of Southern Continental Italy, the number and characteristics of gauged river sections monitored by the SIMN, once data reliability test were carried out. Although Southern Continental Italy corresponds to about one fifth of the whole national surface area, the available data are only 50. Table 1 also shows index floods for each basin, namely the expected value, μ_Q, computed as an arithmetic mean of annual peak floods over the number of year of recorded data; this was preferred to the modal value, since the former is coupled with the extreme probability distribution widely used in Italy, named TCEV (Two-Component Extreme Value) model (Rossi et al., 1984). However, using the modal value would be equally suitable, since it's closely related to the mean. In order to estimate time of concentration, T_C, the Giandotti formula (Eq. 4) (Giandotti, 1934), most commonly used in Italy, was adopted. ARF, previously defined in Eq. (3), was estimated with the empirical formula of Eagleson (1972) (Eq. 5) by using the dimensional coefficients C_1, C_2 and C_3 calibrated for Southern Continental Italy basins (Versace et al., 1989; Rossi, Villani, 1994; Claps et al., 1994). Equation (5) does not depend on the return period whose effect is still negligible in the investigated basins (Rossi, Villani, 1994).

$$T_C = \frac{4\sqrt{A} + 1.5L}{0.8\sqrt{H_m - H_0}} \tag{4}$$

$$\mathrm{ARF}(A,d) = 1 - (1 - e^{-C_1 A}) \cdot e^{-C_2 d^{C_3}} \tag{5}$$

where: (i) T_C is the watershed concentration time (in h); (ii) A is the drainage basin area (in km^2); (iii) L is the length of the longest watercourse to the drainage basin outlet (in km); (iv) H_m is the mean drainage basin elevation (in m); (v) H_o is the drainage basin outlet elevation (in m).

Because the VAPI project provides the IDF Curves for maximum point rainfall for each region, the expected runoff coefficient φ_o, for each watershed, was computed by inverting Eq. (2) and considering $d = T_C$:

$$\varphi_o = \frac{\mu_Q}{\mathrm{ARF}(A,T_C) \cdot \mu[I_P(T_C)] \cdot A} \tag{6}$$

where $\mu[I_P(T_C)]$ is the expected value of IDF curve for maximum point rainfall.

3 Problem definition

Although the computed φ_o values contain errors due to different causes including the specific rainfall-runoff model adopted as well as the reliability of hydrological data measurement, they were assumed to be the most precise estimations that could be obtained with the available data; hence, they will be referred to as "observed runoff coefficient" φ_o.

HESSD
9, 4919–4941, 2012

Since these values definitely depend on soil permeability, the geological formations outcropping in each watershed and the corresponding land cover were defined, in order to give each of these combinations a permeability assessment identified through the "estimated runoff coefficient" value, φ_e, by minimizing the objective function of error:

$$E = \sum_{i=1}^{N} (\varphi_{o,i} - \varphi_{e,i})^2 \tag{7}$$

where N is the number of gauged basins, $\varphi_{o,i}$ and $\varphi_{e,i}$ are, respectively, the mean observed and estimated runoff coefficients for watershed i; the latter is defined by Eq. (8):

$$\varphi_{e,i} = \frac{\sum_{j=1}^{J} \varphi_{e,j} \cdot A_j}{A_i} \tag{8}$$

where $\varphi_{e,j}$, representing the unknown parameter in the objective function Eq. (7), is the estimated runoff coefficient value for every elementary area A_j, characterized by a specific combination of geological formations outcropping and land cover, and J is the total number of elementary areas within each watershed A_i.

The adopted Hydrogeological Map of Southern Italy (Allocca et al., 2007), properly modified by inserting pyroclastic rock cover within some areas of Campania Region (Rasulo et al., 2009), defines four levels of hydrogeological units permeability (Fig. 1). In addition, land covers were derived from the Corine (COoRdination of INformation on Environment) Land Cover digital maps (Bossard et al., 2000) with reference to satellite images of 2000.

However, the number of estimated runoff coefficients given by the combinations of hydrogeological units permeability and land cover previously determined is much greater (136) than the number of experimental data (50). This implies the least squares method of Eq. (7) cannot be used because the system is underdetermined. Instead, an independent permeability classification measure had to be taken into account, in order to reduce the unknowns and to find a relationship between the soil permeability measure and the runoff coefficient.

4 Soil permeability characterization

One of the most widely used classifications of soil permeability and land cover has been proposed by the Soil Conservation Service (SCS, 1972). According to SCS, a single parameter, namely the Curve Number CN, can be used to describe soil permeability, ranging between 0, meaning a highly permeable soil, and 100, meaning a totally impervious surface. Alternatively, a different parameter can be used, that is the maximum potential retention S (in mm), which is related to CN by Eq. (9):

$$S = 254\left(\frac{100}{\mathrm{CN}} - 1\right) \quad (9)$$

Unlike CN, S has a physical interpretation, meaning the maximum water level each soil can retain in accordance to its characteristics. SCS classifies soils in four Hydrological Soil Groups (HSG) A, B, C, D, with a decreasing permeability level from A to D (SCS, 1972). For each HSG, S-values can vary depending on land uses, land treatments, hydrological conditions and antecedent moisture conditions (AMC), the latter corresponding to the rainfall depth in the five days preceding each flood event. The four levels of hydrogeological units permeability of the Hydrogeological Map (Allocca et al., 2007) were supposed corresponding to the SCS Hydrological Soil Groups (A = high, B = moderate, C = low and D = very low infiltration rates), so that each Southern Italian hydrogeological unit could be assigned to a HSG (Table 2). Subsequently, Corine land cover values (34 in the gauged watersheds of the whole number observed in the whole Southern Continental Italy) were cross-combined with the land use/land cover provided by SCS (21 of the SCS total number were used). The proposed mapping is given in Table 3. To carry out the matching operation, some already studied correspondences between SCS and Corine land uses were taken into account (Mancini et al.,

HESSD
9, 4919–4941, 2012

1989; Miliani et al., 2011). When S was found to vary, for the same land use, among all the possible different land treatments and hydrological conditions, the mean value was considered; this was performed because land treatments are more variable in time than land uses, whereas hydrological conditions can not be known on such a large scale. Furthermore, since the purpose of the procedure is not to identify the soil permeability during a particular rainfall event, but only to grade the relative soil permeability, the S-values corresponding to the normal (average) AMC II condition were adopted. Table 4 provides the S-values (in mm), as a classification of the different soil permeability for each hydrologic soil group and land cover, whereas Fig. 2 shows the S map for Southern Continental Italy.

It must be noticed that the Corine map was assumed to be representative of the whole period in which the annual peak flood data were collected in the gauged river sections of the drainage basins shown in Table 1. However, this assumption is not restrictive because (i) the effect of urbanization and therefore the increase in impervious surfaces do not affect soil permeability, given their limited extension with respect to natural basins, (ii) the massive reforestation works occurred during the last postwar period have caused a change in land use from "pastures" to "woods", with an overall negligible increase in the values of potential maximum retention S.

5 Relationship between runoff coefficient and maximum potential retention

Once the multiple combinations of hydrogeological formations and land cover were expressed in a permeability scale, by using the S-value, the existence of its correlation with the runoff coefficient was investigated, with reference to every single elementary area j. The correlation is expressed by the following exponential relationship:

$$\varphi_{e,j} = e^{\alpha S_j + \gamma} \quad (10)$$

where S_j is the maximum potential retention value of each elementary area, whereas α (in mm^{-1}), and γ, dimensionless, are the fitting parameters. A linear relationship

HESSD
9, 4919–4941, 2012

was considered at first, but was rejected since it provides unmeaningful values such as $\varphi > 1$ and $\varphi < 0$ for extreme S-values. The exponential Eq. (10) causes $\varphi = 0$ for $S \to \infty$, but $\varphi > 1$ for $S \to 0$; when φ was found to be greater than 1, it was manually set as equal to 1. The nonlinear objective function (Eq. 7) was solved using the Genetic Algorithm (GA) implemented in GANetXL (Optimization Add-in for Microsoft Excel) (Savić et al., 2011). The fitting procedure provides $\alpha = 0.0175\,\text{mm}^{-1}$ and $\gamma = 0.4428$. The coefficient of determination relative to the 1:1 line in Fig. 3 is $R^2 = 0.387$; in the same figure, $\pm\sigma$ error bands are also drawn, with σ being the standard deviation of observed runoff coefficients, equal to 0.174. The poor fitting rate, that is a rather high value of the unexplained variance, demonstrates that hydrogeological formations and land cover are not the only factors affecting the runoff coefficient.

6 Effect of the climatic index on runoff coefficient

Climate variability indirectly impacts upon the mechanisms of flood generation through the seasonality of rainfall and evapotranspiration, which thus affect the antecedent moisture conditions of a watershed for each single storm event (Sivapalan et al., 2005). Differently, the S-values in Eq. (10) do not account for this effect because they correspond to a homogeneous antecedent moisture condition (AMC II) for all soils of the basins. However, SCS provides S-values for different antecedent soil moisture conditions, higher for dry soil moisture, lower for moist soil moisture. Thus a suitable improvement of Eq. (10) could be achieved correcting S-values by using an appropriate antecedent soil moisture condition. Since in this paper the mean values of annual maximum flood-peak discharges were considered, the greater or lower soil moisture, with respect to any uniform average condition, could be taken into account by adopting a climatic index differentiating the various zones of the gauged watersheds in relation to the higher or lower values of rainfall and temperature. One of the most simple climatic indexes literature provides is Lang's Pluviofactor LF (Lang, 1915):

HESSD
9, 4919–4941, 2012

$$\mathrm{LF} = p/t \tag{11}$$

where p is the mean annual precipitation over a watershed (in mm), and t is the mean annual temperature (in °C).

Using rainfall and temperature data measured during the period 1961–1990, available on the SCIA system web site (National System for the collection, processing and diffusion of climatic data of Environmental Interest – http://www.scia.sinanet.apat.it), a map of the Lang Factor was drawn for Southern Continental Italy, as shown in Fig. 4. The above mentioned period was considered representative of the mean climatic conditions of the whole period in which the annual peak flood data were collected.

A mean value LF_i for each watershed (Table 1), and a mean value LF_M for Southern Continental Italy, equal to 70.25 mm °C^{-1}, were computed. For watersheds with $\mathrm{LF}_i < \mathrm{LF}_M$ potential retention S is expected to increase if compared to the mean moisture condition, whereas for watersheds with $\mathrm{LF}_i > \mathrm{LF}_M$ it is expected to decrease; changes in S will be slighter the smaller is the difference between LF_i and LF_M. Thus, Eq. (10) can be improved as follows:

$$\varphi_{e,j} = e^{\alpha S'_j + \gamma} \tag{12}$$

where S'_j is the new S-value of every elementary area j, corrected by means of its Lang Factor:

$$S'_j = S_j \cdot \left[1 + \frac{\beta}{\alpha}(\mathrm{LF}_i - \mathrm{LF}_M)\right] \tag{13}$$

with all the symbols defined previously. Minimizing the objective function (Eq. 7) provides $\alpha = -0.0266\,\mathrm{mm}^{-1}$, $\beta = 2.26 \times 10^4\,\mathrm{mm}^{-2}\,°\mathrm{C}$ and $\gamma = 1.1897$. The observed and estimated runoff coefficients are shown in Fig. 5 with the $\pm\sigma$ error bands, with σ being the standard deviation of observed runoff coefficients, equal to 0.174. The improved relation has a coefficient of determination $R^2 = 0.553$ relative to the 1:1 line in Fig. 5.

HESSD
9, 4919–4941, 2012
Factors affecting the runoff coefficient
G. Del Giudice et al.

7 Conclusions

Results show that the proposed mapping between the combination of Hydrogeological Map of Southern Italy with the Corine Land Cover and the potential maximum retention S proposed by SCS is physically based. The corrected S-values, improved by means of a climatic index, give a soil permeability scale which is consistent with the SCS scale, thoroughly widespread in engineering applications. Moreover, the S-values are well related with the runoff coefficient, which is a crucial parameter for the index flood estimation within ungauged watersheds.

A rather high value of residual variance can be explained as due to the errors both in discharge measurements in gauged watershed and in the model predictions, and to a general lack of data and overall information on the soil drainage conditions. Since these errors can be neither erased nor taken into account, the proposed results were found to give a significant improvement in a great variety of technical applications. At this aim, Fig. 6 shows a map of the estimated runoff coefficient for Southern Continental Italy carried out by using Eq. (12).

References

Allocca, V., Celico, F., Celico, P., De Vita, P., Fabbrocino, S., Mattia, C., Monacelli, G., Musilli, I., Piscopo, V., Scalise, A. R., Summa, G., and Tranfaglia, G.: Note illustrative della carta idrogeologica dell'Italia Meridionale, Istituto Poligrafico e Zecca dello Stato, Rome, Italy, 2007 (in Italian).

Bossard, M., Feranec, J., and Otahel, J.: CORINE land cover technical guide – Addendum 2000, European Environment Agency Technical report No. 40, Copenhagen, Denmark, 2000.

Chow, V. T., Maidment, D. R., and Mays, L. W.: Applied Hydrology, McGraw-Hill Book Company, New York, 1988.

Claps, P., Copertino, V. A., and Fiorentino, M.: Analisi regionale dei massimi annuali delle portate al colmo di piena, Valutazione delle piene in Puglia, edited by: Copertino, V. A. and

Fiorentino, M., DIFA-University of Basilicata and CNR-GNDCI, Potenza, Italy, 1994 (in Italian).
Cunnane, C.: Methods and merits of regional flood frequency analysis, J. Hydrol., 100, 269–290, 1988.
Dalrymple, T.: Flood frequency analysis, Water Supply Paper 1543-A, US Geol. Survey, Reston, Virginia, USA, 1960.
Eagleson, P. S.: Dynamics of flood frequency, Water Resour. Res., 8, 878–898, 1972.
Giandotti, M.: Previsione delle piene e delle magre dei corsi d'acqua, Memorie e studi idrografici, Pubbl. 2 del Servizio Idrografico Italiano, 8, 107 pp., 1934 (in Italian).
Hosking, J. R. M. and Wallis, J. R.: Regional Frequency Analysis: An Approach Based on L-Moments, Cambridge University Press, Cambridge, 1997.
Koutsoyiannis, D. and Manetas, A.: A mathematical framework for studying rainfall intensity-duration-frequency relationships, J. Hydrol., 206, 118–135, 1998.
Lang, R.: Versuch einer exakten Klassifikation der Boden in klimatischer und geologischer Hinsicht, Int. Mitteil. Bodenk., 5, 312–346, 1915 (in German).
Mancini, M. and Rosso, R.: Using GIS to assess spatial variability of SCS Curve Number at the basin scale, New Directions for Surface Water Modeling, IAHS Publication No. 181, 435–444, IAHS Press Willingford, 1989.
Miliani, F., Ravazzani, G., and Mancini, M.: Adaptation of precipitation index for the estimation of antecedent moisture condition in large Large Mountainous Basins, J. Hydrol. Eng., 16, 218–227, 2011.
Penta, A., Rasulo, G., and Rossi, F.: Criteri di similitudine idrologica per l'analisi dei massimi annuali di pioggia, Proc. CIGR Conf., Florence, Italy, 1972 (in Italian).
Rasulo, G., Del Giudice, G., and Calcaterra, D.: Flood index assessment, Relation between runoff coefficient and the SCS Soil-Cover Complexes, L'Acqua, 2, 37–44, 2009 (in Italian).
Riggs, H. C.: Regional analysis streamflow characteristics, US Geological Survey Water Resources Invest. Tech. Book 4, 1973.
Rossi, F. and Versace, P.: Criteri e metodi per l'analisi statistica delle piene, Valutazione delle Piene, CNR – P. F. Conservazione del Suolo, Publ. No. 165, 63–130, Rome, Italy, 1982 (in Italian).
Rossi, F. and Villani, P.: Valutazione delle Piene in Campania, CNR-GNDCI, Publ. No. 1472, Grafica Matelliana and C., Cava de' Tirreni (SA), Italy, 1994 (in Italian).

HESSD
9, 4919–4941, 2012

Factors affecting the runoff coefficient

G. Del Giudice et al.

Rossi, F., Fiorentino, M., and Versace, P.: Two-component extreme value distribution for flood-frequency analysis, Water Resour. Res., 20, 847–856, 1984.
Savić, D. A., Bicik, J., and Morley, M. S.: A DSS Generator for Multiobjective Optimisation of Spreadsheet-Based Models, Environ. Modell. Softw., 26, 551–561, 2011.
Sivapalan, M., Blöschl, G., Merz, R., and Gutknecht, D.: Linking flood frequency to long-term water balance: incorporating effects of seasonality, Water Resour. Res., 41, W06012, 2005.
Soil Conservation Service (SCS): Section 4: Hydrology, US National Engineering Handbook, US Department of Agriculture, Washington, DC, 1972.
Versace, P., Ferrari, E., Fiorentino, M., Gabriele, S., and Rossi, F.: Valutazione delle Piene in Calabria, CNR-IRPI and GNDCI, Geodata, Cosenza, Italy, 1989 (in Italian).

HESSD
9, 4919–4941, 2012

Table 1. Characteristics of investigated watersheds.

Region	Id	Gauged river section	A (km^2)	Events	μ_Q ($m^3 s^{-1}$)	L (km)	H_m (m)	H_o (m)	T_C (h)	s (%)	φ_o	LF ($mm\,°C^{-1}$)
Calabria	1	Esaro a La Musica	533	19	328.8	37.6	496	49	8.8	1.2	0.44	84.48
	2	Coscile a Camerata	304	29	80.4	26.7	725	58	5.3	2.7	0.12	82.59
	3	Trionto a Difesa	32	16	8.7	9.0	1118	983	3.9	1.0	0.06	75.55
	4	Lese a Schiena D'Asino	61	12	19.0	21.2	1120	687	3.8	2.9	0.08	80.62
	5	Tacina a Rivioto	78	25	81.2	23.3	1332	300	2.7	3.6	0.19	80.59
	6	Alli a Orso	45	47	16.7	19.6	1076	450	2.8	2.6	0.07	88.12
	7	Melito a Olivella	41	16	17.2	17.3	863	369	2.9	3.3	0.08	84.04
	8	Corace a Grascio	178	38	151.7	35.0	820	84	4.9	1.8	0.27	85.54
	9	Ancinale a Razzona	116	50	82.4	24.2	880	514	5.2	1.1	0.16	87.13
	10	Alaco a Mammone	15	19	13.6	3.9	1051	965	2.9	1.3	0.13	88.84
	11	Alaco a Pirrella	38	13	15.6	14.2	893	237	2.2	2.7	0.05	85.34
	12	Duverso a S. Giorgia	29	13	12.9	10.5	971	359	1.9	8.6	0.07	72.36
	13	Metramo a Castagnara	20	12	6.4	4.5	1007	800	2.1	3.5	0.05	85.56
	14	Metramo a Carmine	233	12	73.1	26.9	516	29	5.7	1.7	0.12	77.22
	15	Amato a Marino	115	26	79.2	31.8	758	149	4.6	1.7	0.23	84.17
	16	Lao a Piè di Borgo	280	23	211.2	20.3	832	270	5.1	1.8	0.33	93.94
Basilicata	17	Bradano a S. Giuliano	1658	17	539.1	100.8	440	69	20.4	0.4	0.44	46.44
	18	Bradano a Ponte Colonna	462	31	184.1	53.0	560	215	11.1	0.6	0.36	49.28
	19	Basento a Menzena	1403	24	405.6	127.1	664	20	16.8	0.5	0.33	53.84
	20	Basento a Gallipoli	860	31	359.8	51.5	893	400	11.0	1.0	0.38	58.30
	21	Basento a Pignola	44	28	36.9	12.5	1074	742	3.1	3.7	0.32	64.15
	22	Agri a Tarangelo	511	32	188.7	37.6	870	470	9.2	0.8	0.25	87.02
	23	Agri a Le Tempe	174	27	84.5	18.4	933	585	5.4	1.5	0.25	85.65
	24	Sinni a Valsinni	1141	28	497.1	69.3	752	150	12.2	0.9	0.30	72.30
	25	Sinni a Pizzutello	233	34	234.2	32.2	932	446	6.2	1.6	0.54	96.71
Puglia	26	Canale S. Maria	58	16	18.0	17.7	201	90	6.8	1.3	0.22	49.51
	27	Ofanto a S. Samuele di Cafiero	2716	47	517.6	142.1	454	32	25.7	0.3	0.44	51.97
	28	Ofanto a Cairano	266	23	208.0	32.2	674	380	8.3	0.7	0.66	72.60
	29	Ofanto a Monte Verde Scalo	1017	50	431.2	56.0	657	270	13.4	1.0	0.63	62.62
	30	Lavello	124	32	45.1	18.8	530	4	4.0	3.0	0.17	52.24
	31	Venosa a Ponte S. Angelo	264	28	61.9	39.3	502	199	8.9	0.8	0.21	48.17
	32	Locone a Ponte Brandi	220	10	40.3	22.0	340	137	8.1	1.0	0.15	43.40
	33	Carapelle a Carapelle	715	36	277.4	76.6	510	50	12.9	0.3	0.51	48.23
	34	Cervaro a Incoronata	540	52	217.3	78.5	379	51	14.5	0.7	0.54	52.45
	35	Candelaro a Strada di Bonifica 24	1778	9	158.1	60.5	240	10	21.4	0.3	0.19	48.23
	36	Celone a S. Vincenzo	93	17	34.2	23.8	532	188	5.0	2.1	0.18	55.69
	37	Celone a Ponte Foggia-S. Severo	237	37	43.2	43.8	380	61	8.9	1.1	0.16	51.44
	38	Vulgano a Ponte Troia-Lucera	94	20	72.9	22.2	486	170	5.1	2.1	0.38	56.28
	39	Salsola a Casanova	44	19	45.1	16.6	444	184	4.0	2.6	0.43	55.28
	40	Casanova a Ponte Lucera-Motta	57	18	25.7	15.2	474	178	3.9	2.2	0.19	53.89
	41	Salsola a Ponte Foggia-S. Severo	456	40	74.5	47.2	235	39	14.0	0.9	0.23	51.38
	42	Triolo a Ponte Lucera-Torremaggiore	56	17	38.5	22.0	302	109	5.7	1.4	0.41	50.39
Campania	43	Volturno ad Amorosi	1950	41	636.3	114.1	540	35	19.3	0.4	0.45	92.04
	44	Calore Irpino ad Apice	548	38	325.0	48.5	607	153	9.8	1.0	0.50	75.41
	45	Tammaro a Paduli	660	19	213.5	69.2	597	125	11.9	0.7	0.38	66.13
	46	Calore Irpino a Solopaca	2968	15	995.0	106.2	536	47	21.3	0.4	0.62	69.99
	47	Volturno a Ponte Annibale	5493	16	1296.8	146.3	534	17	28.4	0.3	0.47	77.46
	48	Tusciano ad Olevano sul Tusciano	104	10	40.4	19.5	940	133	3.1	4.5	0.08	86.49
	49	Tanagro a Polla	628	50	213.1	56.9	812	431	11.9	0.5	0.30	100.93
	50	Alento a Casalvelino	286	18	261.4	28.3	350	5	7.4	0.7	0.58	90.74

Main characteristics of river basins involved in the analysis are: basin area A; number of available events N; mean of maximum annual peak flood (index flood) μ_Q; length of the longest watercourse to the basin outlet L; mean basin altitude H_m (m a.s.l.); minimum basin altitude H_o (m a.s.l.); time of concentration computed using the Giandotti equation T_C; average watershed slope s; Lang Factor LF; observed runoff coefficient φ_o. River basins with at least 10 events were used for analysis.

HESSD

9, 4919–4941, 2012

Factors affecting the runoff coefficient

G. Del Giudice et al.

Table 2. Correspondence between Hydrogeological complexes and Hydrological Soil Groups.

Hydrogeological Units	Unit permeability (HSG)
Alluvial-coastal	B
Lake	C
Continental Epiclastic sediments	B
Travertine	A
Calabrian "Alteriti"	B
Pyroclastic-fall deposits	B
Pyroclastic-flow deposits	B
Lava	A
Sand-Conglomerate	B
Clay	D
Molassic sediments	B
Messina Evaporites	B
Sandstone-Conglomerate	B
Sandstone-Limestone-Pelite Succession	C
Limestone-Pelite Succession	C
Transitional Calcarenite-Marl	B
Apulia Platform Limestone	A
Limestone from Mount Marzano Unit and Maddalena Mountains Unit	A
Dolomite from Maddalena Mountains and Mount Foraporta Unit	B
Limestone from Alburno-Cervati-Pollino Unit	A
Dolomite from Alburno-Cervati Pollino Unit	B
Dolomite from Bulgheria-Verbicaro Unit	B
Limestone from San Donato Unit Metamorphi	B
Silicate-Marl from Lagonegro Unit I and II	C
Limestone with Flint from Lagonegro Unit I and II	B
Marl-Sandstone-Pelites from Molise Unit	C
Limestone-Marl from Molise Unit	B
Metapelite-metacalcareous Frido Unit	C
Ophiolite from Frido Unit	C
Limestone-Clay from North-Calabrian Unit	B
Clay-Limestone from Sicilian Unit	D
Igneous Rocks	B
Metamorphic Rocks	C
Fractured Metamorphic Rocks	B
Limestone	C
Surface Water	D
Limestone from Matese-Mount Maggiore and Monte Alpi Unit	A
Lim. with Pyroclastic cover from Matese-M. Magg. and M. Alpi Unit	B
Dolomite from Matese-Mount Maggiore and Monte Alpi Unit	B
Dol. with Pyroclastic cover from Matese-M. Maggiore and M. Alpi Unit	C
Limestone from Picentino-Taburno Unit	A
Limestone with Pyroclastic cover from Picentino-Taburno Unit	B
Dolomite-Marl from Picentino-Taburno Unit	B
Dolomite-Marl with Pyroclastic cover from Picentino-Taburno Unit	C
Limestone from Bulgheria-Verbicaro Unit	A
Limestone with Pyroclastic cover from Bulgheria-Verbicaro Unit	B

HESSD
9, 4919–4941, 2012

Table 3. Correspondence between Corine Land Cover and SCS land uses.

CORINE Code	CORINE Land Cover Description	S.C.S. Land Use Description
1.1.1	Continuous Urban Fabric.	Urban districts (commercial and business).
1.1.2	Discontinuous Urban Fabric.	Residential districts by average lot size (1/8 acre or less).
1.2.1	Industrial or commercial units.	Industrial districts.
1.2.2	Road and rail networks and associated land.	Paved streets and roads; curbs and storm drains.
1.2.4	Airports.	Residential districts by average lot size (1/8 acre or less).
1.3.1	Mineral extraction sites.	Herbaceous mixture of grass, weeds and low-growing brush (poor HC).
1.3.2	Dump sites.	Herbaceous mixture of grass, weeds and low-growing brush (poor HC).
1.3.3	Construction sites.	Developing urban areas.
1.4.1	Green urban areas.	Open space (poor HC).
1.4.2	Sport and leisure facilities.	Open space (fair HC).
2.1.1	Non-irrigated arable land.	Small grain.
2.1.2	Permanently irrigated land.	Close-seeded legumes or rotational meadows.
2.2.1	Vineyards.	Row crops.
2.2.2	Fruit rees and berry plantations.	Woods-grass combination.
2.2.3	Olive groves.	Woods-grass combination.
2.3.1	Pastures.	Herbaceous mixture of grass, weeds and low-growing brush (good HC).
2.4.1	Annual crops associated with permanent crops.	Woods-grass combination (poor HC).
2.4.2	Complex cultivation patterns.	Close-seeded legumes or rotational meadows.
2.4.3	Land principally occupied by agriculture, with significant areas of natural vegetation.	Woods-grass combination.
2.4.4	Agro-forestry areas.	Woods-grass combination.
3.1.1	Broad-leaved forest.	Woods.
3.1.2	Coniferous forest.	Woods.
3.1.3	Mixed forest.	Brush-brush-weed-grass mixture.
3.2.1	Natural grasslands.	Open space (good HC).
3.2.2	Moors and heathlands.	Pinyon, juniper or both with grass understory.
3.2.3	Sclerophyllous vegetation.	agebrush with grass understory.
3.2.4	Transitional woodland-shrub.	Sagebrush with grass understory (fair HC).
3.3.1	Beach, dunes, sands.	Saltbush, greasewood, creosote-bush,blackbrush, bursage, palo verde, mesquite and cactus.
3.3.2	Bare rocks.	Saltbush, greasewood, creosote-bush,blackbrush, bursage, palo verde, mesquite and cactus.
3.3.3	Sparsely vegetated areas.	Saltbush, greasewood, creosote-bush,blackbrush, bursage, palo verde, mesquite and cactus.
3.3.4	Burnt areas.	Saltbush, greasewood, creosote-bush,blackbrush, bursage, palo verde, mesquite and cactus.

HC = Hydrologic Condition. All kinds of wet land cover are not placed in this table.

HESSD
9, 4919–4941, 2012

Table 4. Maximum potential retention S (mm) according to HSG and land uses.

CORINE code	S (mm) according to Hydrological Soil Group			
	A	B	C	D
1.1.1	31	22	16	13
1.1.2	76	45	28	22
1.2.1	60	35	25	19
1.2.2	5	5	5	5
1.2.4	76	45	28	22
1.3.1	114	64	38	19
1.3.2	114	64	38	19
1.3.3	76	41	25	16
1.4.1	397	162	89	64
1.4.2	264	114	68	48
2.1.1	156	94	60	45
2.1.2	169	99	60	48
2.2.1	125	80	52	41
2.2.2	323	137	76	56
2.2.3	323	137	76	56
2.4.2	169	99	60	48
2.4.3	323	137	76	56
2.4.4	323	137	76	56
2.3.1	381	156	89	45
2.4.1	192	94	56	41
3.1.1	432	169	94	64
3.1.2	432	169	94	64
3.1.3	493	275	192	149
3.2.1	120	68	41	31
3.2.2	323	184	94	64
3.2.3	397	244	149	109
3.2.4	452	244	149	109
3.3.1	200	99	56	41
3.3.2	200	99	56	41
3.3.3	200	99	56	41
3.3.4	200	99	56	41

HESSD
9, 4919–4941, 2012

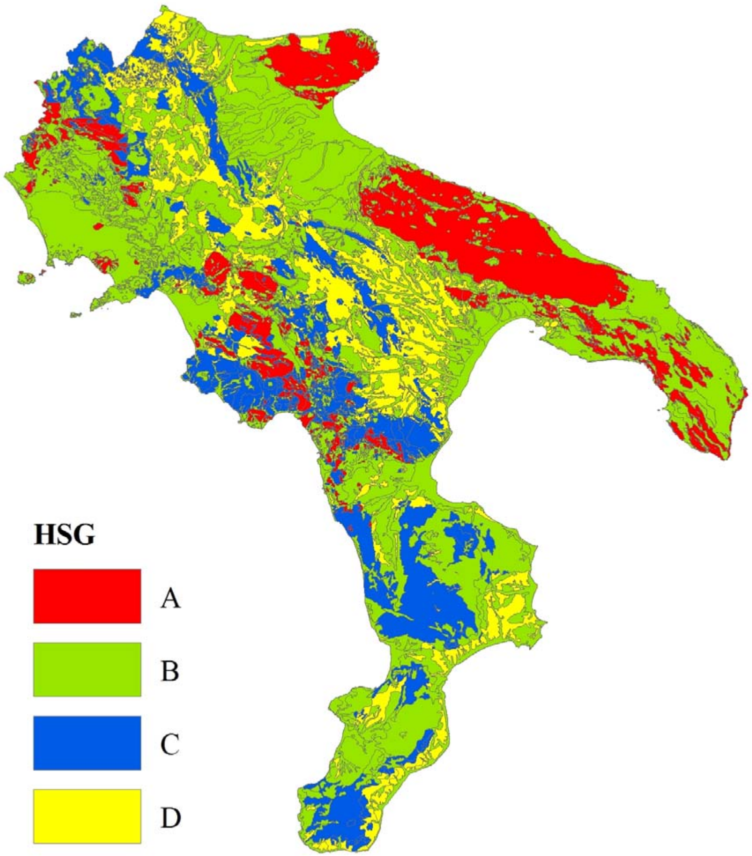

Fig. 1. Hydrologic Soil Groups within Southern Continental Italy.

HESSD
9, 4919–4941, 2012

Factors affecting the runoff coefficient

G. Del Giudice et al.

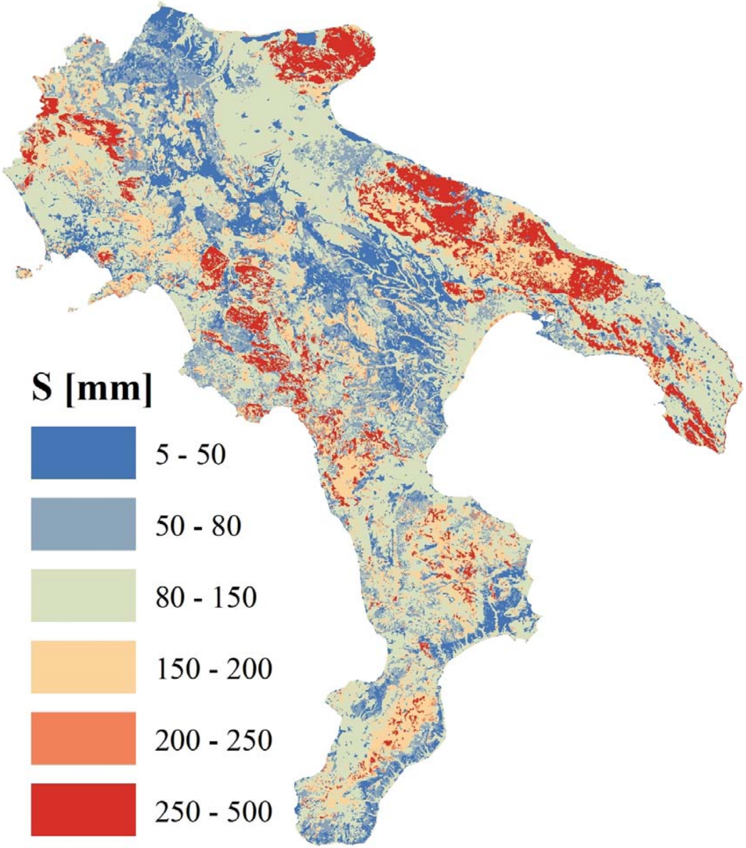

Fig. 2. Potential Maximum Retention *S* within Southern Continental Italy.

HESSD
9, 4919–4941, 2012

Title Page
Abstract | Introduction
Conclusions | References
Tables | Figures
◀I | ▶I
◀ | ▶
Back | Close
Full Screen / Esc
Printer-friendly Version
Interactive Discussion

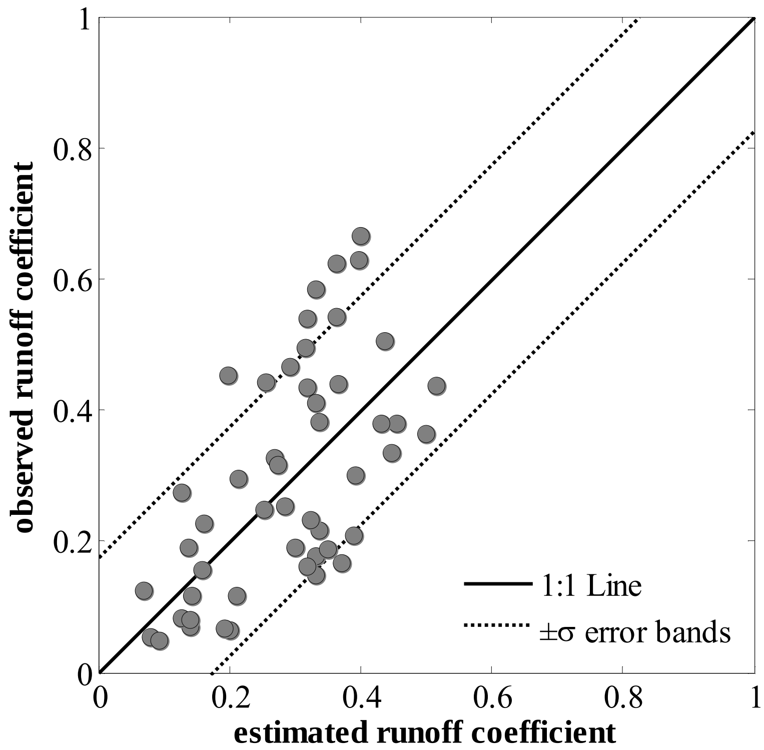

Fig. 3. Observed and estimated values of runoff coefficient by considering the potential maximum retention effect. Standard deviation σ of observed data is 0.174.

HESSD
9, 4919–4941, 2012

Factors affecting the runoff coefficient

G. Del Giudice et al.

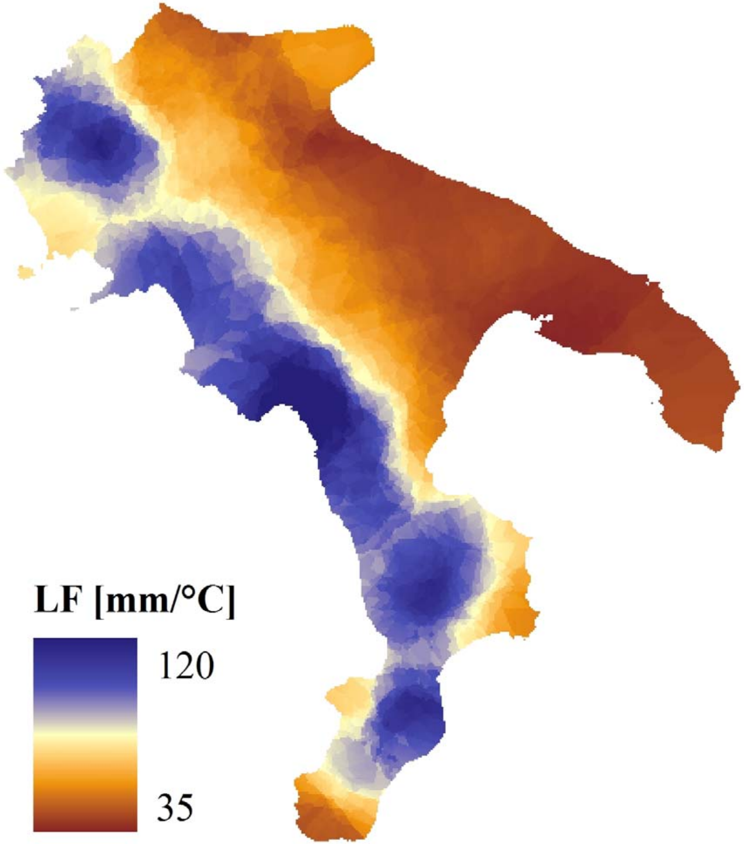

Fig. 4. Lang Factor within Southern Continental Italy.

HESSD
9, 4919–4941, 2012

Factors affecting the runoff coefficient

G. Del Giudice et al.

Title Page
Abstract Introduction
Conclusions References
Tables Figures
◀I ▶I
◀ ▶
Back Close
Full Screen / Esc
Printer-friendly Version
Interactive Discussion

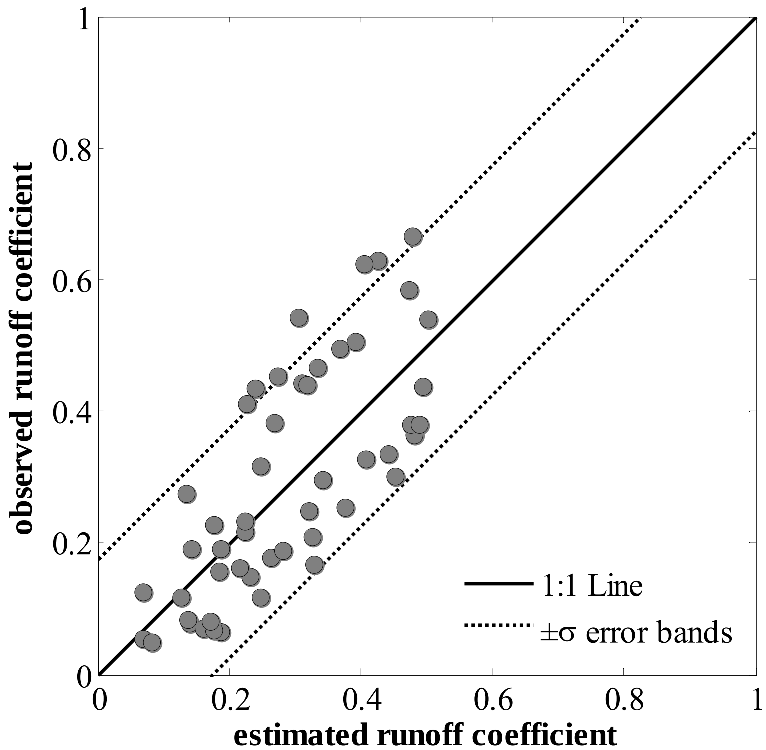

Fig. 5. Observed and estimated values of runoff coefficient by considering both the potential maximum retention and the climate effects. Standard deviation σ of observed data is 0.174.

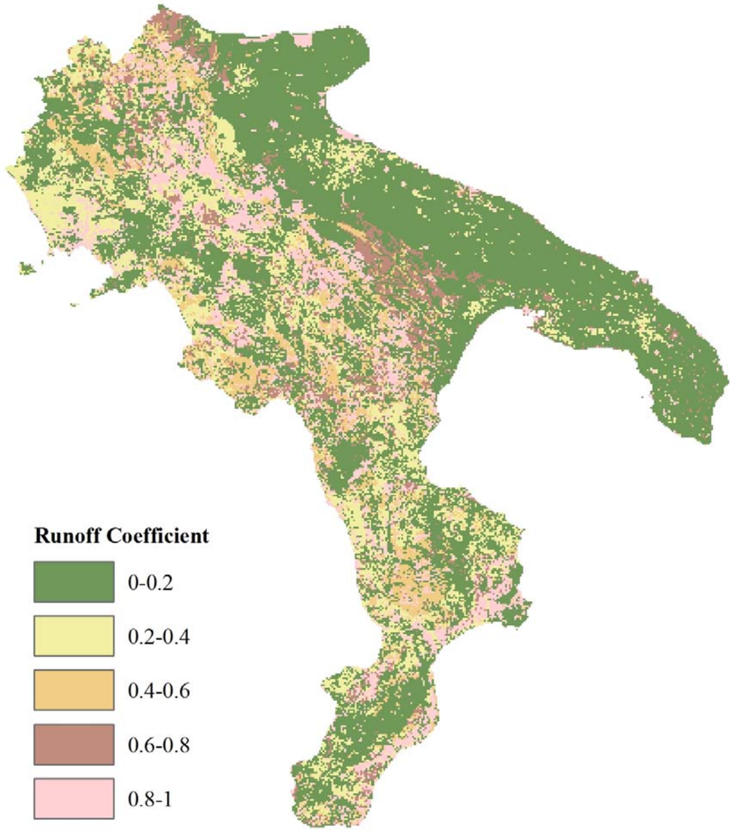

Fig. 6. Runoff coefficient map within Southern Continental Italy.

HESSD
9, 4919–4941, 2012